PHYSICAL REVIEW A VOLUME 26, NUMBER 5 NOVEMBER 1982

Tjon effect for dense systems. A molecular-dynamics study

J. J. Brey, J. Gómez Ordóñez, and A. Santos
Departamento de Física Teórica, Facultad de Física, Universidad de Sevilla, Sevilla, Spain
(Received 26 April 1982)

The time evolution of an isolated, spatially homogeneous system, with an isotropic distribution of velocities and with particles interacting via a Lennard-Jones potential, has been analyzed by means of molecular dynamics. The initial velocity distribution is assumed to be zero except for two given speeds v_α and v_β. We have found an overpopulation phenomenon for high speeds, analogous to the one observed in the theoretical studies of model Boltzmann equations. The influence of v_α and v_β on this effect has been analyzed. A qualitative comparison with theoretical results is presented. Furthermore, we have observed a similar, less intense, overpopulation effect for low speeds.

I. INTRODUCTION

A few years ago, Bobylev[1] and, independently, Krook and Wu[2] found a particular exact solution of the nonlinear Boltzmann equation for a homogeneous gas with an isotropic velocity distribution, whose molecules interact via a repulsive Maxwell potential, i.e., a potential depending upon the fourth power of the intermolecular distance. The original Bobylev-Krook-Wu solution (the so-called BKW mode) corresponds to some special initial conditions, while the general solution can be expressed in terms of a Laguerre series.[3] These results have motivated a great interest for the nonlinear Boltzmann equation and its exact solutions.[4]

By solving numerically the Boltzmann equation for a two-dimensional model with Maxwellian interaction, Tjon[5] has found that, for some initial states, the relaxation towards equilibrium of the distribution function is not monotonic. The corresponding high-energies part of the distribution function, that was initially zero, builds up quickly over the equilibrium values and then decays to it from above. This overpopulation phenomenon, absent in the BKW mode, seems to be important when one tries to evaluate rate constants for chemical or thermonuclear reactions. Alexanian[6] and Hauge[7,8] have suggested a criterion to discern which initial distributions lead to a relaxation towards equilibrium from above for the high-energy tail. Evidently, it is interesting to check whether real systems show this overpopulation phenomenon or, by contrast, it only shows up in highly simplified models far away from real situations.

In this paper, we present the results of a molecular-dynamical simulation of the relaxation towards equilibrium of an isolated, homogeneous system with an isotropic velocity distribution. The particles interact via a Lennard-Jones potential. The initial velocity distribution function consists of two delta peaks, as considered by Tjon[5] and others.[7–9]

This paper is organized as follows. In Sec. II we describe the initial conditions and introduce the notation. The method used to generate the initial distribution is discussed in Sec. III. We also check that the simulated system is really isolated, in the sense that its energy remains constant in time, and is homogeneous. In Sec. IV, the results obtained are presented and analyzed. The conclusions arising from them are rather qualitative, due to the reduced number of particles that can be handled in a molecular-dynamical simulation. Nevertheless, those results show that, for a given temperature, and for sufficiently distant delta peaks, the overpopulation phenomenon observed by Tjon for high speeds does really appear. At the same time a similar phenomenon, not mentioned in the literature to the best of our knowledge, is observed for low speeds.

II. INITIAL CONDITIONS

As we said in the Introduction, the overpopulation effect was first found by Tjon[5] when extending previous calculations of Tjon and Wu.[9] These authors consider a system of Maxwell molecules ini-

tially described by a distribution function homogeneous in space and isotropic in the velocities. Furthermore, it vanishes except for the two speeds v_α and v_β given. The overpopulation effect appears then for certain values of v_α and v_β. Mathematically, such an initial distribution can be written as

$$f(v;0)=N[c_\alpha\delta(v-v_\alpha)+c_\beta\delta(v-v_\beta)] , \quad (2.1)$$

where N is the number of particles in the system and c_α, c_β are given by

$$c_\alpha=\frac{v_\beta^2-3}{v_\beta^2-v_\alpha^2} , \quad (2.2)$$

$$c_\beta=\frac{3-v_\alpha^2}{v_\beta^2-v_\alpha^2} . \quad (2.3)$$

These constants have been determined through the conditions

$$\int_0^\infty dv\, f(v;0)=N , \quad (2.4)$$

$$\int_0^\infty dv\, v^2 f(v;0)=3N . \quad (2.5)$$

We have taken as the velocity unit $(k_B T_0/m)^{1/2}$, k_B being the Boltzmann constant, m the mass of each particle, and $\frac{3}{2}k_B T_0$ the initial kinetic energy per particle. In this paper, velocities will always be expressed in terms of this unit.

By convention, we take $v_\alpha<v_\beta$. Then the positivity of the distribution function implies that

$$v_\alpha\le\sqrt{3}\le v_\beta . \quad (2.6)$$

Let us introduce the function $\varphi(v_1,v_2;t)$ representing the number of particles whose speeds are between v_1 and v_2 at time t. From the Maxwell-Boltzmann distribution, the equilibrium expression for φ is given by

$$\varphi^{eq}(v_1,v_2)=N\{\sqrt{2T_0/\pi T}\,[v_1\exp(-v_1^2T_0/2T)-v_2\exp(-v_2^2T_0/2T)] +\mathrm{erf}(v_2\sqrt{T_0/2T})-\mathrm{erf}(v_1\sqrt{T_0/2T})\} , \quad (2.7)$$

where $\mathrm{erf}(x)$ is the error function defined by

$$\mathrm{erf}(x)=\frac{2}{\sqrt{\pi}}\int_0^x dy\, e^{-y^2} . \quad (2.8)$$

In Eq. (2.7), T represents the equilibrium temperature of the system which does not coincide with T_0, as we will discuss later on.

To characterize the system relaxation towards equilibrium, we introduce the function

$$R(v_1,v_2;t)=\frac{\varphi(v_1,v_2;t)}{\varphi^{eq}(v_1,v_2)} . \quad (2.9)$$

This function must, of course, tend to unity for $t\to\infty$, for any pair of values of v_1 and v_2.

III. SIMULATION METHOD

A system of $N=864$ particles with periodic boundary conditions and with a Lennard-Jones

$$u(r)=4\epsilon\left[\left[\frac{\sigma}{r}\right]^{12}-\left[\frac{\sigma}{r}\right]^{6}\right] \quad (3.1)$$

interaction potential has been simulated through the use of molecular dynamics.[10] The particles are initially distributed with a fcc structure. The length of the unit cell side is $(4/\rho)^{1/3}$, where ρ is the number density of particles. The equations of motion are numerically integrated through the use of a time step

$$h=0.032(m\sigma^2/48\epsilon)^{1/2}$$

equivalent to 10^{-14} s for Ar. The lattice structure ensures the initial spatial homogeneity for volume elements containing several unit cells.

The initial velocity distribution function is obtained in the following way. We generate three random numbers ξ_i, η_i, and ζ_i in the interval [0,1] for each particle i. The components of the velocity of particle i are

$$\begin{aligned} v_{ix}&=v_i\sin(\pi\eta_i)\cos(2\pi\zeta_i) , \\ v_{iy}&=v_i\sin(\pi\eta_i)\sin(2\pi\zeta_i) , \\ v_{iz}&=v_i\cos(\pi\eta_i) . \end{aligned} \quad (3.2)$$

By this procedure we ensure that no privileged direction exists and therefore the initial distribution can be considered isotropic. The other random number ξ_i is used to determine the speed of particle i. To simulate the distribution (2.1), v_i is taken to be v_α if $\xi_i\le c_\alpha$ and v_β if $\xi_i>c_\beta$. Notice that we assign either value for the speed of particle i, independent of its spatial location.

Given a set of $3N$ independent random numbers $\{\xi_v,\eta_i,\zeta_i\}$, the vector velocity of each of the N particles is determined by this algorithm. In other words, in this way we define a particular microstate of the macrostate defined by the distribution (2.1). Nevertheless, we expect that the time evolution of each microstate can be used to characterize the evo-

lution of the macrostate when dealing with a coarse-grained description, which is the type of description considered here.

To clarify this point, we have generated two microstates corresponding to two different sets of random numbers by applying the algorithm described above. We have then followed the time evolution of each microstate. In Fig. 1 we represent $R(0.0,0.9;t)$ and $R(3.1,\infty;t)$ for $v_\alpha=1$ and $v_\beta=3$ starting from two different microstates. It can be observed in this figure that the essential features of the evolution show up simultaneously in both microstates. More concretely we refer to the initial build up until the equilibrium value is crossed, the maximum overpopulation and the further relaxation towards equilibrium. We notice a better agreement for speeds in the interval $0\leq v\leq 0.9$ than for $v\geq 3.1$. This is due, basically, to the greater absolute population in the first interval; actually,

$$\varphi^{\mathrm{eq}}(0.0,0.9)\simeq 164$$

and

$$\varphi^{\mathrm{eq}}(3.1,\infty)\simeq 8\ .$$

This justifies that fluctuations of $R(3.1,\infty;t)$ are much bigger than those of $R(0.0,0.9;t)$. For this reason, we do not represent the final relaxation stage to equilibrium for $R(3.1,\infty;t)$ in Fig. 1. These difficulties, arising from the reduced number of particles of our model, will appear in all our results. So our conclusions will have a mainly qualitative character. In fact, we have carried out a study of the statistical error on the functions R shown in Fig. 1 by considering several initial microstates. In this way, we have estimated a typical error of 5% for $R(0.0,0.9;t)$, but for $R(3.1,\infty;t)$ we have found values of the order of 15%. Of course, the statistical error depends on the region of speeds under consideration.

In order to analyze the influence of the values of v_α and v_β on the relaxation to equilibrium, we have studied the cases corresponding to the following values of (v_α,v_β): (1,2), (1,3), (1,4), and (1,5), all of them with the conditions $\rho\sigma^3=0.60$ and $k_BT_0/\epsilon=3.00$.

The simulated system is isolated and then the total energy must remain constant in time. As a check of this, we show in Fig. 2 the time evolution of the total energy per particle E and the kinetic energy per particle K for the pair (1,4). We can observe that E remains, indeed, constant. Nevertheless, the kinetic contribution to the total energy decreases until a stationary value K_{st} is reached. This value allows us to define an equilibrium temperature T from the relation $K_{\mathrm{st}}=\frac{3}{2}k_BT$. This is the temperature used to define the function $\varphi^{\mathrm{eq}}(v_1,v_2)$ given by Eq. (2.7). This equilibrium temperature is not exactly the same for all pairs studied by us. It varies between $2.46\epsilon/k_B$ and $2.61\epsilon/k_B$. This variation does not affect our analysis at all.

In the models studied with the Boltzmann equation[4] the kinetic energy remains constant because

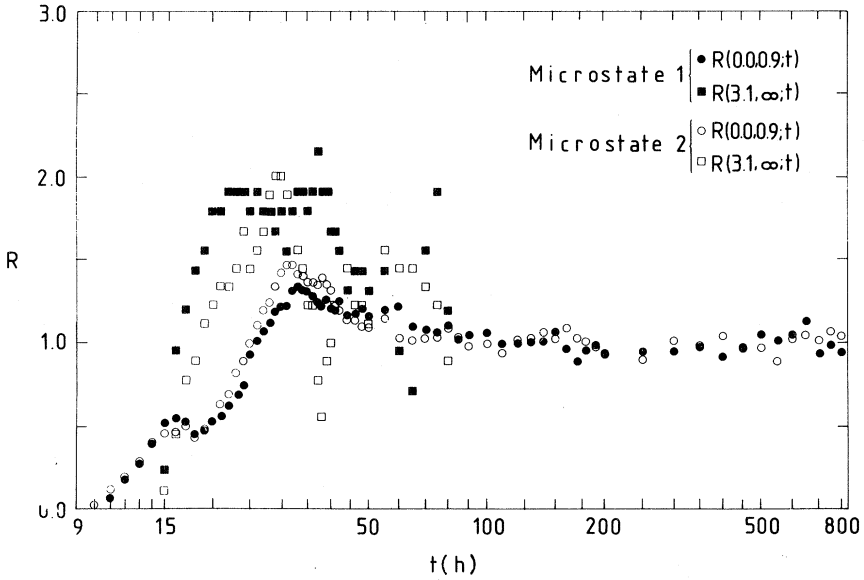

FIG. 1. Relative population vs time for the pair $(v_\alpha,v_\beta)=(1,3)$ starting from two different initial microstates. Circles correspond to speeds lower than v_α and the squares to speeds higher than v_β.

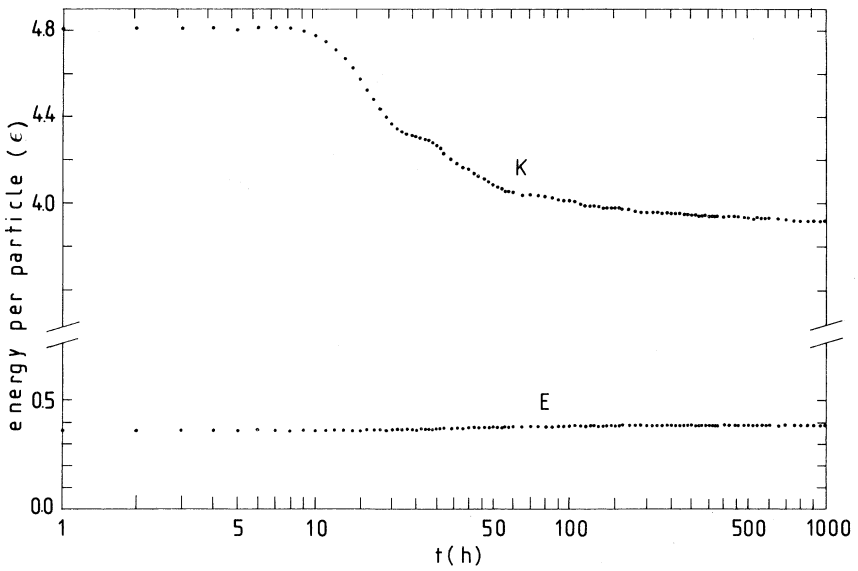

FIG. 2. Time evolution of the total energy per particle (E) and the kinetic energy per particle (K) for the pair (v_α, v_β)=(1,4).

there is no potential energy contribution. On the other hand, we study a moderately dense gas and, therefore, the potential energy is not only non-negligible but, as shown in Fig. 2, it is of the same order (in absolute value) as the kinetic energy.

In agreement with distribution (2.1), the initial K should be $\frac{3}{2}k_BT_0=\frac{9}{2}\epsilon$. But our results show that, for $t\to 0^+$, $K\simeq 4.8$. This is due to the fact that the fraction of particles with speed v_α does not exactly coincide with the theoretical value c_α as a consequence of the finite number of particles in our system. Of course, the number of particles with speed v_β is affected in the same manner.

It is also interesting to determine on what degree the system is really homogeneous. We then split the system in l layers of thickness half the side of the unit cell. For our values of N and ρ, $l=12$. In each layer j, we measure the number of particles n_j and the kinetic energy $\hat{K}_j$. The values of n_j/n and $\hat{K}_j/\hat{K}$ for the pair (1.5) are represented in Fig. 3 for different times. Here, $n=N/l$ and $\hat{K}=Kn$. Because of our initial spatial configuration (fcc structure) and the thickness of our layers, $n_j=n$ for all j at the initial time. As time evolves, n_j oscillates around its average value with an average fluctuation of 4%. As for the kinetic energy $\hat{K}_j$, we observe that fluctuations are more important. In particular, for $t=0$ the fluctuations are of 29%, and later, they stabilize at 11% for $t\gtrsim 50$ h. The reason for the rather large value of the initial flucuations of $\hat{K}_j$ is again related with the limited number of particles in each layer ($n=72$). A small variation of the number of particles with speed v_β in a layer gives rise to an appreciable deviation of $\hat{K}_j$ from $\hat{K}$. Therefore, the kinetic energy fluctuations in each layer will be bigger the greater the difference between v_α and v_β is. Notice that the case represented in Fig. 3 corresponds to the biggest value of v_β considered by us.

It is also observed in Fig. 3 that there is a certain correlation between the fluctuations of n_j and $\hat{K}_j$. This is so because the kinetic energy in each layer is related to the number of particles in the same layer.

IV. RESULTS

After discussing the reliability of our simulation method, we proceed to present the results obtained. In Fig. 4 we represent

$$R(v-\Delta v,v;t)$$

versus v at different t. The graph corresponds to the pair (1,3) and $\Delta v=0.1$. We do not consider speeds greater than 3.6 because, due to the smallness of Δv, the populations in the intervals corresponding to high speeds are so small that fluctuations of R become very big. Zero population points cannot be represented in our logarithmic scale of R.

For $t=15$ h the influence of the initial conditions is still clearly observed. The time sequence shows that the peak corresponding to v_β decays faster than the one corresponding to v_α during the initial stage. We will come back to this point later. The last time represented corresponds practically to an equilibri-

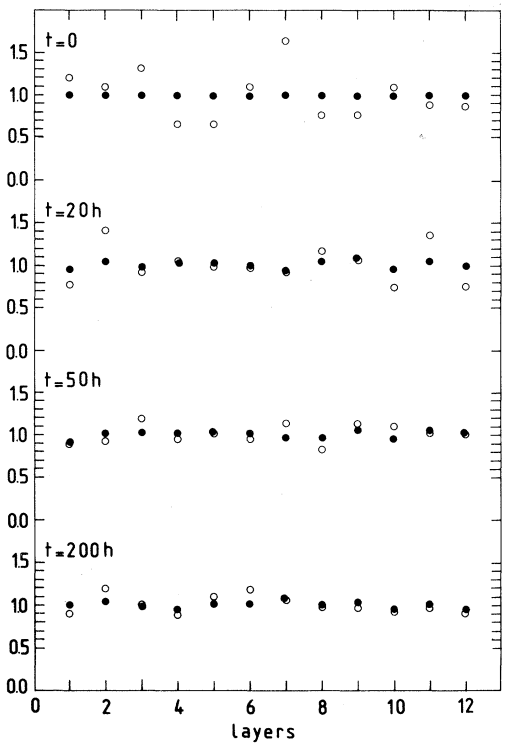

FIG. 3. Ratios n_j/n (solid circles) and $\hat{K}_j/\hat{K}$ (circles) for each layer j for the pair $(v_\alpha,v_\beta)=(1,5)$ at different times; n_j is the number of particles of layer j, $\hat{K}_j$ is the kinetic energy of layer j, and n and $\hat{K}$ are their average values.

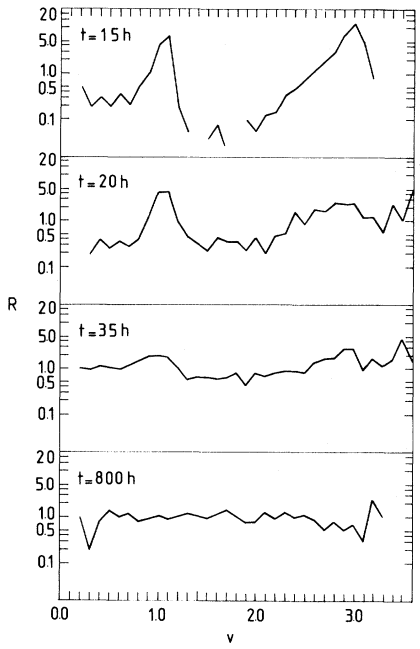

FIG. 4. Relative population vs speed at different times for $(v_\alpha,v_\beta)=(1,3)$.

um situation. Because the populations are much smaller at the tails than at the central region, there the fluctuations of R about unity are important.

Neglecting the fluctuations, it follows from Fig. 4 that the relaxation towards equilibrium is not monotonic, but first the particle population crosses its equilibrium value, decaying to it afterwards. This overpopulation effect appears basically for speeds slightly smaller than v_α or v_β, the effect being more pronounced the closer the speed to v_α or v_β is. Consequently, an asymmetry in the evolution of $R(t)$ for speeds very close to those peaks exists. This is because, initially, particles with speeds v_α or v_β tend to decelerate in such a way that most of the particles having speeds between v_α and v_β at a later time initially had the speed v_β. This effect is not to be understood as the Tjon overpopulation phenomenon for high speeds.[5] For the remaining pairs (v_α,v_β) studied, an analogous behavior has been observed with a greater overpopulation the greater v_β is.

To carry out a more detailed analysis of the overpopulation effect, we have studied the behavior of $R(v_1,v_2;t)$ for speeds close to v_α and v_β. Figure 5

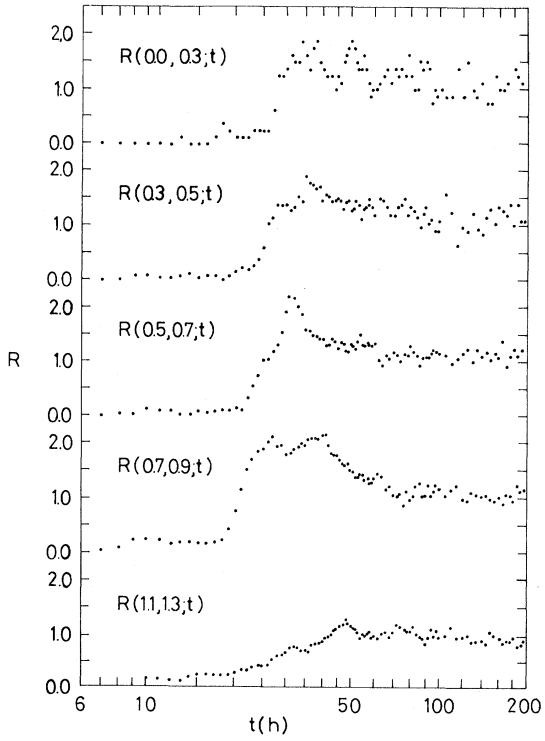

FIG. 5. Time evolution of the relative population for speeds close to v_α in the case (1,5).

shows R versus t for speeds close to v_α for the pair (1,5). The comments referred to Fig. 4 are more clearly seen in this Fig. 5. In particular, the asymmetry between $R(0.7,0.9;t)$ and $R(1.1,1.3;t)$ for speeds slightly smaller and bigger than v_α, respectively, is confirmed. The population for speeds greater than v_α increases monotonously until reaching its equilibrium value, without any significant overpopulation effect. On the other hand, the population for speeds smaller than v_α, after an initial stage when it practically vanishes, increases rapidly, crossing over the equilibrium value, and then decaying to it at a later time. Furthermore, the overpopulation shows up sooner and with greater strength the closer the speed is to v_α.

A similar analysis shows the same features for the remaining pairs considered by us. But we have observed that the overpopulation for speeds lower than v_α appears sooner and more intense when the value of v_β increases. For instance, for the pair (1,2), a relevant overpopulation appears only for $0.7 \leq v \leq 0.9$. To the best of our knowledge, this overpopulation for speeds lower than v_α has not been previously observed by the authors dealing with model nonlinear Boltzmann equations.[4] In this sense, we think that this point deserves a further theoretical elaboration.

Next, we study the behavior for speeds close to v_β. The curves obtained for the pair (1,3) are shown in Fig. 6. As it happened near v_α, a clear asymmetry between $R(2.7,2.9;t)$ and $R(3.1,3.3;t)$ exists. For speeds slightly greater than v_β, the overpopulation is almost undetectable. Nevertheless, for speeds slightly smaller than v_β, the effect is clearly observed. This overpopulation appears later, being less intense the smaller the speed is. In fact, for speeds in the interval $2.3 \leq v \leq 2.5$ the relaxation to equilibrium is monotonic. The same conclusions are reached for the pair (1,2). However, the overpopulation effect shows up at a later time and with less strength. For instance, the maximum value of $R(1.7,1.9;t)$ is roughly 1.6 and the overpopulation starts at $t \simeq 12$ h, while there is no significant overpopulation for the interval $1.5 \leq v \leq 1.7$. The pairs (1,4) and (1.5) are much less clear, due to the fact that the number of particles with speeds close to v_β is so small that fluctuations disguise the mean behavior. For instance,

$$\varphi^{\text{eq}}(3.9,4.1) \simeq 0.28$$

for $T = 2.61\epsilon/k_B$.

Let us now present the analysis of the evolution of populations for high speeds, to check whether in

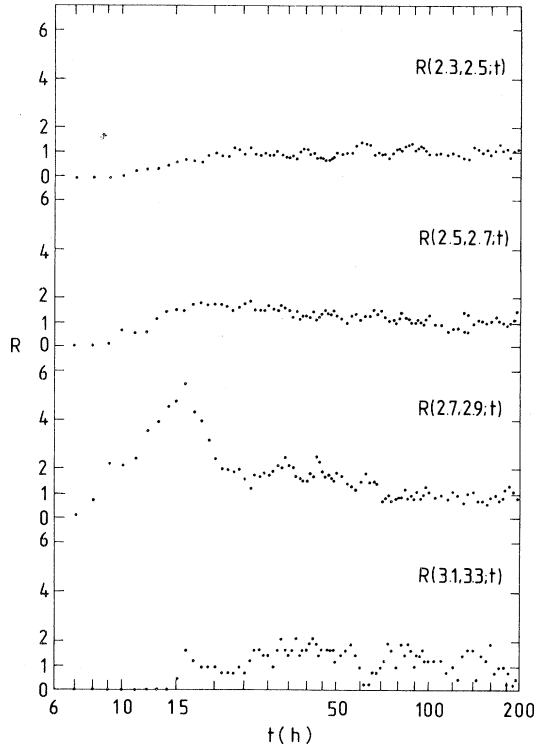

FIG. 6. Time evolution of the relative population for speeds close to v_β in the case (1,3).

our system an analogous phenomenon to the one observed by Tjon[5] exists. Owing to the very low populations in this range of speeds, a detailed study will not be possible. We will then consider globally all speeds greater than v_β.

Figures 7 and 8 represent the time evolution of R for speeds greater than v_β and for the pairs (1,2) and (1,4), respectively. For comparison purposes, we also show in theses graphs the evolution of $R(0.0,0.9;t)$ corresponding to speeds lower than v_α. An analogous representation was presented in Fig. 1. Observe that, while the overpopulation is present for the pairs (1,3) and (1,4) in the considered ranges, it does not appear for (1,2). This seems to indicate that, for a given value of v_α, there exists a value of v_β such that, for v_β greater than this one, overpopulation shows up. This agrees with the theoretical model's results as far as high speeds are concerned. In particular, for the Maxwellian model Boltzmann equation, the criterion of Alexanian[6] and of Hauge[7,8] indicates that overpopulation exists if

$$(v_\beta^2 - 3)(3 - v_\alpha^2) > 6 .$$

This criterion agrees with our conclusion that, for

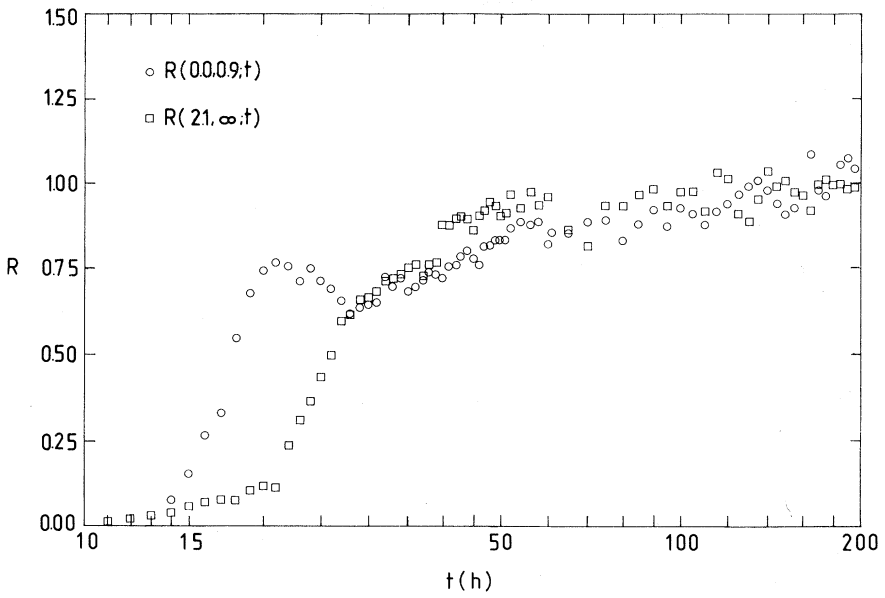

FIG. 7. Time evolution of the relative population for speeds slower than v_α (circles) and faster than v_β (squares) for the pair (1,2).

the pair (1,2), overpopulation is not present, while it exists for the pair (1,3). This is so even when the interaction potential in our system is very different from the Maxwellian one.

From Figs. 1 and 8, we see that the overpopulation is greater and shows up sooner for speeds $v > v_\beta$ than for speeds $v < v_\alpha$. Also, the effect is more appreciable the greater v_β is and it appears more clearly for $v > v_\beta$. The maximum values of $R(0.0,0.9;t)$ and of $R(5.1,\infty;t)$ are 1.87 and 5.4×10^3, respectively, for the pair (1,5). For the pair (1,4) the maximum of $R(0.0,0.9;t)$ is 1.79. The broken lines in Fig. 8 denote that there are points corresponding to a vanishing population which can-

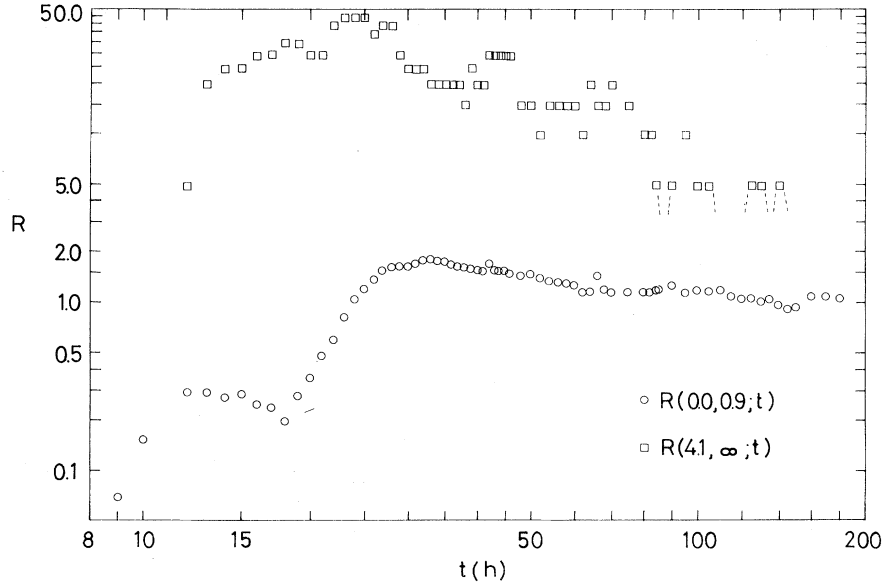

FIG. 8. Time evolution of the relative population for speeds slower than v_α (circles) and faster than v_β (squares) for the pair (1,4).

not be represented. Actually, the lowest represented values correspond to an absolute population of one particle, while

$$\varphi^{eq}(4.1,\infty)\simeq 0.20 .$$

So, in our simulation method, this is the best precision for the fluctuations about equilibrium.

Hauge and Praestgaard[8] have solved the Boltzmann equation for a Maxwell model with the initial distribution (2.1). It is observed in Fig. 1 of Ref. 8 that the maximum overpopulation for the speed $v=6.3$ for the pair (1,3) is $R\simeq 2$, appearing at a time which is about one third of the equilibrium relaxation time. In Fig. 1 of the present paper, the maximum of $R(3.1,\infty;t)$ also appears at a time about one third of the equilibrium relaxation time and its value is roughly 2. We should remark that we have described the speeds higher than v_β globally because the fluctuations do not allow us to study the population for $v\simeq 6$.

Finally, we have studied the equilibrium relaxation of the population corresponding to speed intervals centered at v_α and v_β. Figures 9 and 10 represent such relaxations for the pairs (1,2) and (1,3), respectively. For the pair (1,2), a clear difference between the relaxation times of both populations is not observed. This may be due to the proximity of v_α and v_β. However, for the case (1,3) it is observed that the population corresponding to v_β relaxes more quickly than that of v_α. Although the same behavior seems to be present in the case (1,4), fluctuations forbid us to reach a definitive conclusion and, thus, we do not reproduce this case.

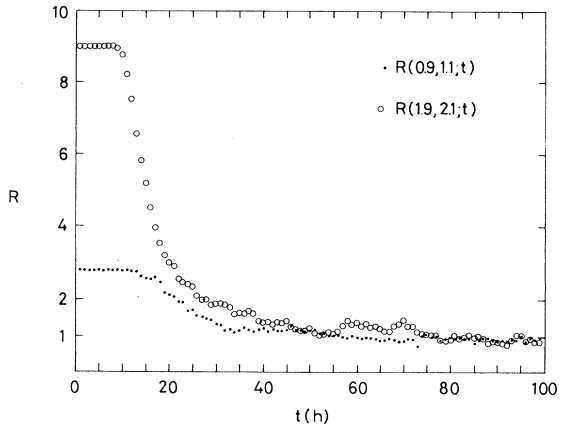

FIG. 9. Time evolution of the relative population for two speed intervals around v_α (dots) and v_β (circles) in the case (1,2).

By numerically solving a two-dimensional Boltzmann equation with Maxwellian interaction, Tjon[5] observed a slower time relaxation for high-energy particles. In particular, for the pair

$$(v_\alpha,v_\beta)=(0.90,2.70) ,$$

the v_α population relaxes sooner than that of v_β. The apparent contradiction between this behavior and the one observed in Fig. 10, might be due to the use of different interaction potentials. Let us recall that in the Maxwell model the collision frequency is

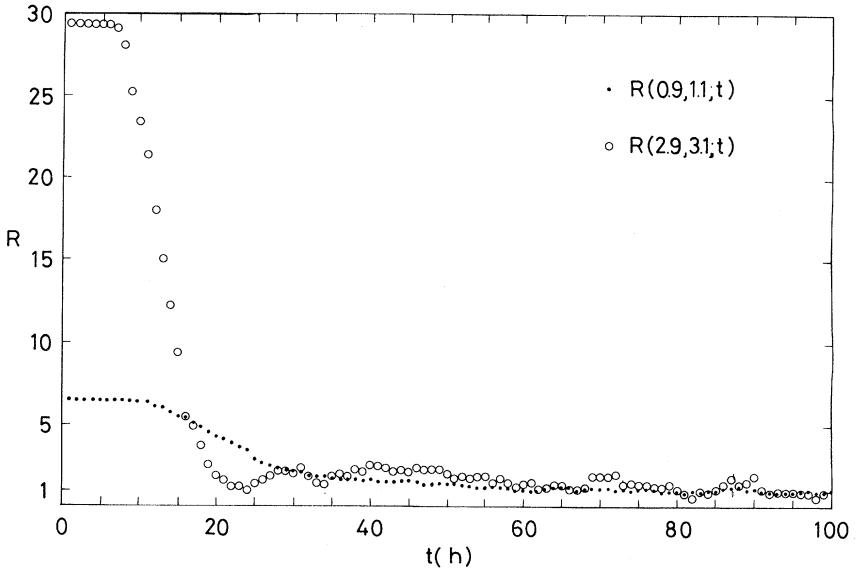

FIG. 10. Time evolution of the relative population for two speed intervals around v_α (dots) and v_β (circles) in the case (1,3).

velocity independent.

Of course, much work remains to be done in this field. In particular, it should be interesting to establish the relevance of the observed effects in the case of a less singular distribution function of speeds. Also, a more explicit relation of this effect with macroscopic phenomena, such as chemical and thermonuclear reactions, would be welcomed.

---

[1]A. V. Bobylev, Dok. Akad. Nauk SSSR 225, 1041 (1975); 225, 1296 (1975); 231, 571 (1976) [Sov. Phys.—Dokl. 20, 820 (1976); 20, 822 (1976); 21, 632 (1976)].
[2]M. Krook and T. T. Wu, Phys. Rev. Lett. 36, 1107 (1976); 38, 991 (1977); Phys. Fluids 20, 1589 (1977).
[3]M. H. Ernst, Phys. Lett. 69A, 390 (1979).
[4]M. H. Ernst, Phys. Rep. 78, 1 (1981).
[5]J. A. Tjon, Phys. Lett. 70A, 390 (1979).
[6]M. Alexanian, Phys. Lett. 74A, 1 (1979).
[7]E. H. Hauge, Phys. Lett. 74A, 183 (1979).
[8]E. H. Hauge and E. Praestgaard, J. Stat. Phys. 24, 21 (1981).
[9]T. Tjon and T. T. Wu, Phys. Rev. A 19, 883 (1979).
[10]See, for example, L. Verlet, Phys. Rev. 159, 98 (1967).